INFRARED SPECTRA OF LUNAR SOILS

By J. R. Aronson, A. G. Emslie, and E. M. Smith

Annual Progress Report
For Period January, 1978, through March, 1979

NAS 9-15356

During the present year's work the infrared spectra of all ten lunar samples have been measured using our Michelson interferometer spectroscopic apparatus. Several of the measurements had to be repeated as the instrumental difficulties encountered early in 1978 led us to suspect that some errors may have been present in our original data. The spectra of the three samples that we repeated are grossly similar to the spectra measured last year except that a long wavelength broad band feature is now much weaker than it appeared in our previous runs for all three samples. The spectra are all presented in the format of brightness temperature versus frequency (Figure 1) as it was shown in our previous work[1] that this format provides suitable contrast and eliminates the difficulties having to do with inexact knowledge of the temperature of the surface of the powder under vacuum conditions. Furthermore, data from a remote sensing mission would undoubtedly be presented in such a format for the same reasons.

As our Michelson interferometer beamsplitter is less efficient at the extremes of the spectral region studied, and as some residual water vapor is not totally compensated for in our measurements, the reliability of the data is reduced near 300 and 1400 cm^{-1}. The measured data were stored in a computer file and several filtering techniques employed in order to discriminate against the noise in the measurements. We finally chose to smooth the data by passing it twice through a digital four-pole Butterworth low-pass filter, once forward and once backward. This process cancels phase shifts which could otherwise distort or displace

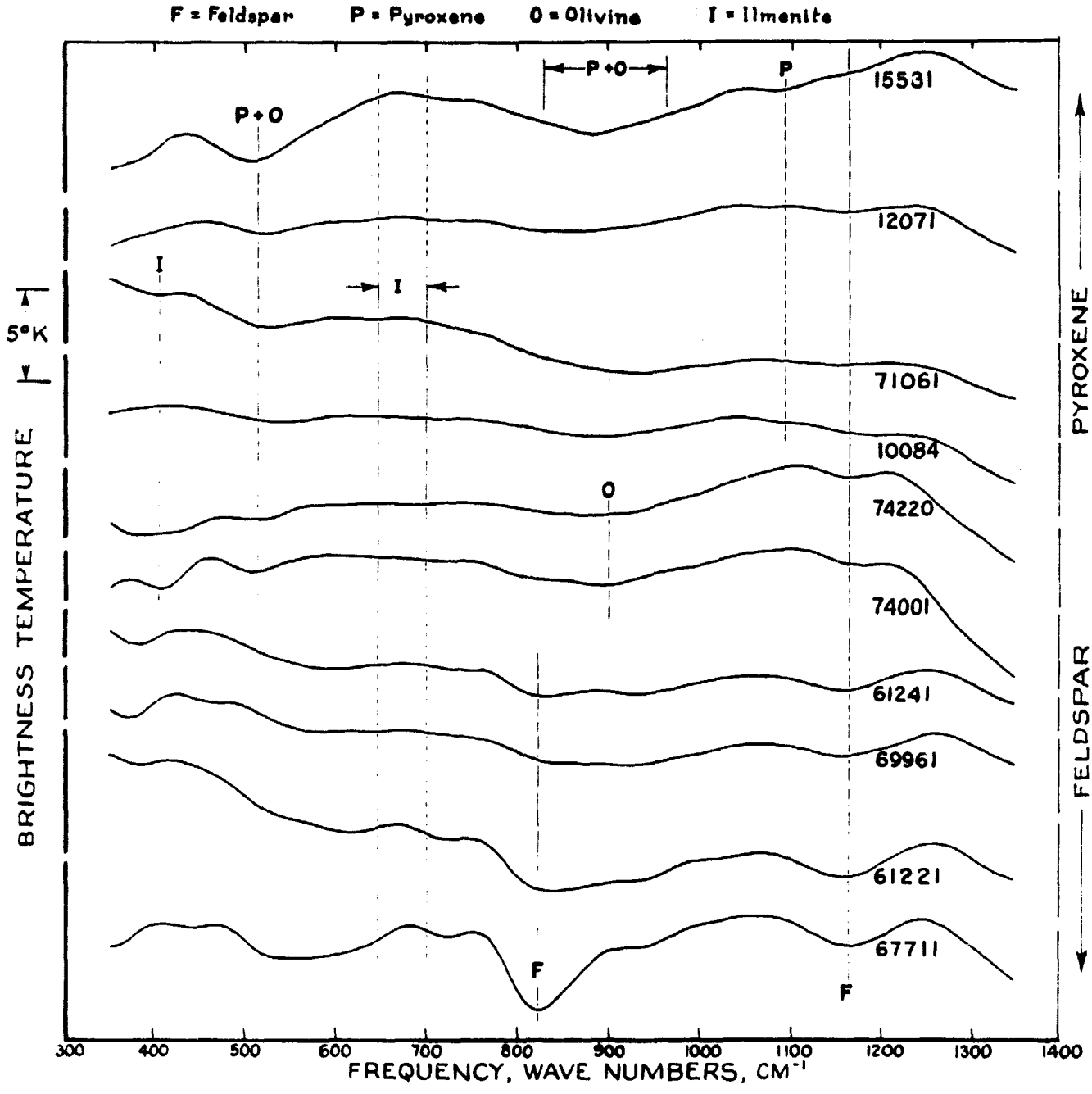

LUNAR SAMPLE SPECTRA

Figure 1

features of the spectrum. The filter cutoff point was set at 80 cm^{-1}. Spectral features having periods shorter than 80 cm^{-1} are attenuated rapidly as the periods decrease, e.g., by a factor of 500 (54 dB) at 40 cm^{-1}. Features having periods longer than 80 cm^{-1} are relatively unaffected, the attenuation being negligible at 160 cm^{-1}. At the cutoff period the attenuation is a factor of 2 (6 dB). The cutoff point was set by comparison with the original data which had been studied to ascertain whether the various features were reproducible. It was chosen so as to minimize the possibility of significantly attenuating any real features while discriminating heavily against features obviously due to noise.

We believe that the apparent tilts in some of the measured data of Figure 1 are artifacts and should be ignored.

In the correlations that follow we have assumed that the normative CIPW values[2,3] are representative of real mineral compositions in lieu of a more complete description. Unfortunately the soil catalog[4] gives mineralogical descriptions only for small size cuts and not for an entire soil sample. Therefore we felt that using the CIPW norms was the most useful procedure. Table I summarizes the CIPW norms for our samples.

The spectra of the various samples show that considerable diagnostic information is present. Several conclusions are immediately apparent. First any sample in which the feldspar content is high has a very distinctive band in the vicinity of 820 cm^{-1}, with a second band near 1170 cm^{-1} also being present. The band near 820 cm^{-1} has been previously shown to result from a relatively transparent region in the spectra of all feldspars and was discussed to some extent in our analog work.[1] Theoretical simulations of the spectra of approximately 5 μm powders show this band clearly when the optical constants of the feldspar are properly derived. It is apparent that the spectra of small particle size simulations more truly represent the spectra of the real particle size distributions than do the spectra of coarse particle simulations despite the fact that the average particle diameter on the lunar surface

TABLE I

	Mol %				
	Feldspar	Pyroxene	Olivine	Ilmenite	I_s/FeO
15531	28.42	57.23	10.25	4.12	27.0
12071	37.93	48.35	7.29	5.37	47.0
71061	30.95	44.03	6.19	17.70	14.0
10084	39.40	43.74	1.92	14.89	78.0
74220	18.95	38.73	23.99	16.73	1.0
74001	18.94	39.07	23.47	16.73	-
61241	71.87	16.46	10.10	1.35	47.0
69961	73.95	15.27	9.42	1.14	92.0
61221	79.02	15.53	4.81	.93	9.2
67711	85.47	7.15	7.19	.49	2.8

is known to be in the vicinity of 60 μm. This is due to the large contribution to the scattering coefficient by the smaller particles which enables them to dominate the spectra. The feldspar features are very clearly visible in samples 67711, 61221, 69961, and 61241 (Figure 1).

Ferromagnesian silicates show a feature between 850 and 950 cm^{-1} that is quite broad as well as a feature centered between 500 and 550 cm^{-1}. In addition pyroxene dominated mixtures show a feature near 1100 cm^{-1}, but that feature is quite weak. If a mixture of pyroxene and olivine minerals occurs that does not show the pyroxene feature at 1100 cm^{-1} and has a peak very near 900 cm^{-1}, the presence of significant olivine is indicated. This is shown in samples 74220 and 74001 (Figure 1). Sample 15531 might have been considered to have high olivine except for the distinctive appearance of the 1100 cm^{-1} feature due to pyroxene, whereas both 74220 and 74001 clearly show the absence of such a feature. Samples 12071 and 10084 show the 1100 cm^{-1} feature to a lesser degree, but it is plainly present in comparison with the feldspar rich samples. Ilmenite has been much more difficult to identify due to the relatively small amounts present and to the fact that all of the silicates have a jumble of features in the region of ilmenite's characteristic bands (between 400 and 550 cm^{-1}). Nonetheless a feature centered near 400 cm^{-1} occurs in three of the four high ilmenite samples (Figure 1). It correlates well with a 410 cm^{-1} feature in pure ilmenite.

In addition we have observed that the four samples containing significant ilmenite (see Table I) can marginally be distinguished from the other six in the spectral region between 650 and 700 cm^{-1}. The ilmenite containing samples have no noticeable feature in this region while the other samples have small but observable maxima (in brightness temperature). This small effect was then confirmed by examination of theoretical simulations and is quite noticeable if the ilmenite content of a theoretical mixture is increased to 40%. It results from the relatively large (ca. 3X compared to silicates) and featureless values of the scattering coefficient of ilmenite in this region.

It is also clear from the data of Figure 1 that the high contrast spectra represent relatively immature soils as is to be expected from the correlation between maturity and agglutinates previously established.[5] The I_s/FeO maturity index[2,5] for our samples is shown in Table I. It is well known that contrast will be reduced if the samples contain a great deal of glass.[1] However, samples 74220 and 74001 show intermediate contrast between the immature soils and mature soils such as 12071 and 10084. The intermediate character of 74220 and 74001 may be explained by their lack of agglutinates. Agglutinates have additional contrast reduction owing to the almost uniform spectral absorption by the tiny metallic particles present. This explanation is presumably also responsible for the higher contrast of 69961 than would be expected judging by its high FMR resonance ratio.

During the course of the present year's work we have obtained better optical constants for ilmenite by measuring a single crystal sample to replace the data previously developed for a polycrystalline ilmenite sample.[6] Optical constants for both the E$\perp$c and E$\parallel$c orientations have been derived from polarized infrared measurements of polished sections of a single crystal supplied to us by Professor Frondel of Harvard University. In addition to this, a single crystal of enstatite was measured in three separate orientations such that the optical constants for the orientations E$\parallel$c, E$\parallel$b, and E$\parallel$a could all be obtained. The resulting Lorentz line parameters[6] are shown in Tables II through VI, and the fits to the data are shown in Figures 2 through 6.

Theoretical simulations of enstatite soil based on these optical constants have been compared to the theoretical simulations based on the diopside and augite samples previously measured. It is apparent that the resulting spectra are so similar that the quantitative differences observable are not likely to be diagnostic in the presence of the signal-to-noise ratios obtainable in remote measurements. We therefore do not believe we will be able to distinguish clino- and

TABLE II - ILMENITE (E⊥c) ε_∞ = 4.8625 (.1731)

ν_j		γ_j		S_j	
670.45	(6.85)	.12318	(.03832)	.04096	(.01513)
508.66	(2.40)	.17096	(.01153)	1.41819	(.15485)
414.18	(1.75)	.12783	(.01053)	3.44629	(.22847)
299.16	(2.23)	.18690	(.01713)	8.15007	(.50707)

TABLE III - ILMENITE (E||c) ε_∞ = 3.2929 (.0891)

ν_j		γ_j		S_j	
679.36	(1.55)	.08408	(.00360)	.22809	(.01182)
500.20	(2.51)	.13151	(.00514)	1.64489	(.19355)
426.93	(12.66)	.18525	(.14544)	.27729	(.32275)
368.00	(3.48)	.06464	(.02420)	.14088	(.06448)
288.74	(12.25)	.08630	(.01479)	1.21204	(.75280)

TABLE IV - ENSTATITE (E||a) ε_∞ = 3.8452 (.1518)

ν_j		γ_j		S_j	
1042.85	(.89)	.00311	(.00075)	.20003	(.01391)
1002.81	(1.38)	.01387	(.00270)	.06552	(.00805)
936.15	(1.65)	.00433	(.00122)	.66463	(.02804)
632.50	(4.64)	.06312	(.01802)	.21750	(.04328)
553.98	(1.20)	.01557	(.00401)	.10473	(.03257)
541.18	(2.53)	.02167	(.02491)	.06119	(.06828)
520.19	(2.80)	.03741	(.01800)	.18305	(.07589)
444.94	(.70)	.00579	(.00559)	.08257	(.02887)
433.17	(1.95)	.03193	(.02142)	.13537	(.11011)
414.79	(3.13)	.04788	(.03712)	.19842	(.19469)
390.66	(6.15)	.09833	(.04017)	.32624	(.20227)
341.02	(1.8[illegible])	.01925	(.01478)	.11842	(.10241)
315.75	(2.49)	.02120	(.00929)	4.53728	(.43197)

TABLE V - ENSTATITE (E||b) ε_∞ = 2.4265 (.1208)

ν_i		γ_i		S_i	
1117.87	(2.62)	.01075	(.00419)	.01106	(.00306)
1026.07	(.77)	.01369	(.00160)	.01256	(.00155)
998.34	(.93)	.01392	(.00331)	.00460	(.00112)
967.11	(.77)	.01137	(.00251)	.01315	(.00304)
926.34	(1.38)	.01899	(.00194)	.20604	(.01713)
855.13	(1.41)	.01813	(.00176)	.28159	(.01298)
741.83	(15.74)	.07019	(.07656)	.04318	(.04090)
681.42	(3.12)	.02170	(.01602)	.03221	(.02074)
647.97	(7.73)	.04304	(.02697)	.02467	(.01653)
564.14	(1.03)	.02427	(.00625)	.02290	(.00753)
533.96	(.53)	.01519	(.00345)	.07373	(.01616)
493.98	(1.24)	.02774	(.00391)	.89432	(.11336)
452.66	(1.68)	.05391	(.00894)	.92530	(.09333)
396.08	(1.88)	.03651	(.01057)	.60313	(.14001)
376.81	(4.34)	.03807	(.07442)	.15725	(.19539)
327.11	(6.79)	.12025	(.09509)	.53257	(.41285)

TABLE VI - ENSTATITE (E||c) ε_∞ = 2.6309 (.0702)

ν_i		γ_i		S_i	
1065.78	(.84)	.01377	(.00065)	.20257	(.01234)
1019.92	(1.19)	.01485	(.00453)	.07950	(.01205)
917.70	(.44)	.01129	(.00141)	.03578	(.00419)
889.52	(.76)	.01425	(.00128)	.20637	(.00790)
726.44	(27.05)	.05490	(.17094)	.02810	(.06666)
723.69	(7.48)	.01110	(.02497)	.01847	(.06858)
671.34	(24.10)	.07710	(.07672)	.04117	(.04878)
565.07	(.80)	.01348	(.00217)	.03142	(.00392)
548.40	(.41)	.02144	(.00275)	.03058	(.00328)
479.05	(.85)	.02432	(.00257)	.93109	(.16256)
463.41	(1.54)	.02741	(.01086)	.33024	(.14990)
378.26	(.65)	.01598	(.00593)	.03200	(.00915)
349.73	(.70)	.03086	(.00236)	.79220	(.03347)

orthopyroxenes without considerably more work. The ilmenite results show that the data obtained from our previous ilmenite polycrystalline sample were sufficiently accurate. The problems with the chemistry of that sample and the approximation of having to assume the sample was homogeneous did not cause very great difficulties in the development of a set of suitable oscillator parameters and hence optical constants.

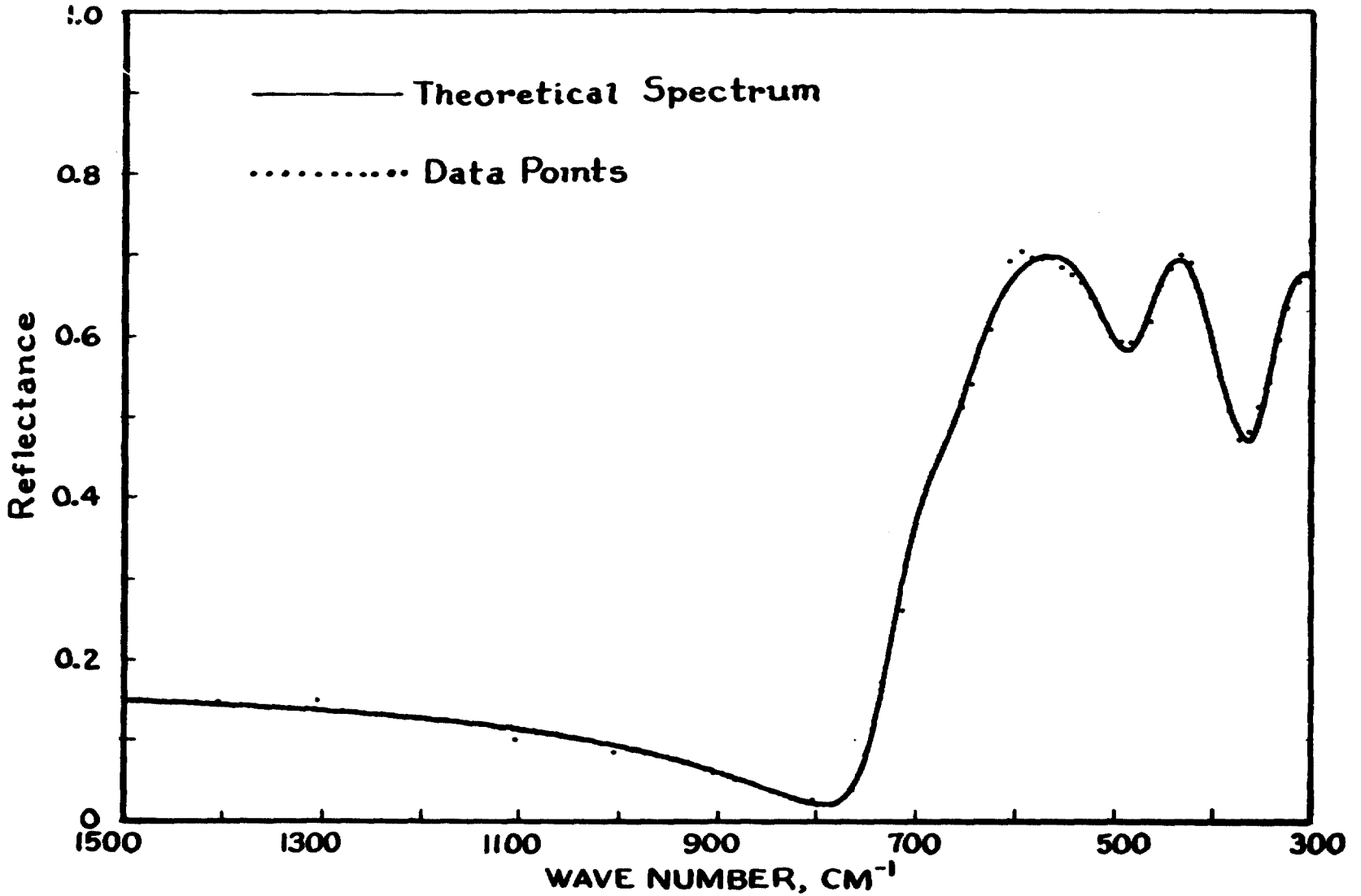

REFLECTANCE SPECTRUM OF ILMENITE (E⊥c) FITTED WITH FOUR LINES

Figure 2

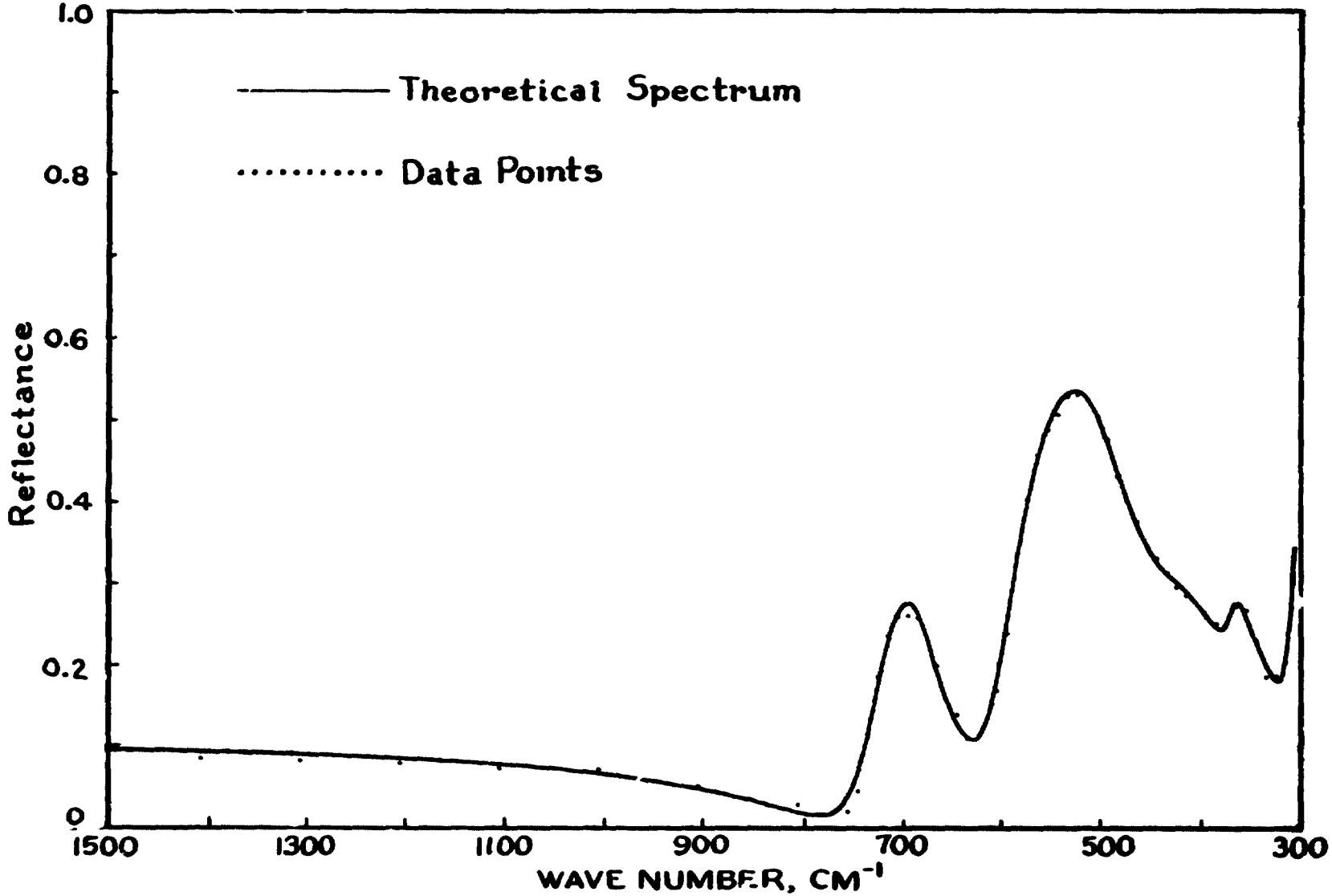

REFLECTANCE SPECTRUM OF ILMENITE (E⊥c) FITTED WITH FIVE LINES

Figure 3

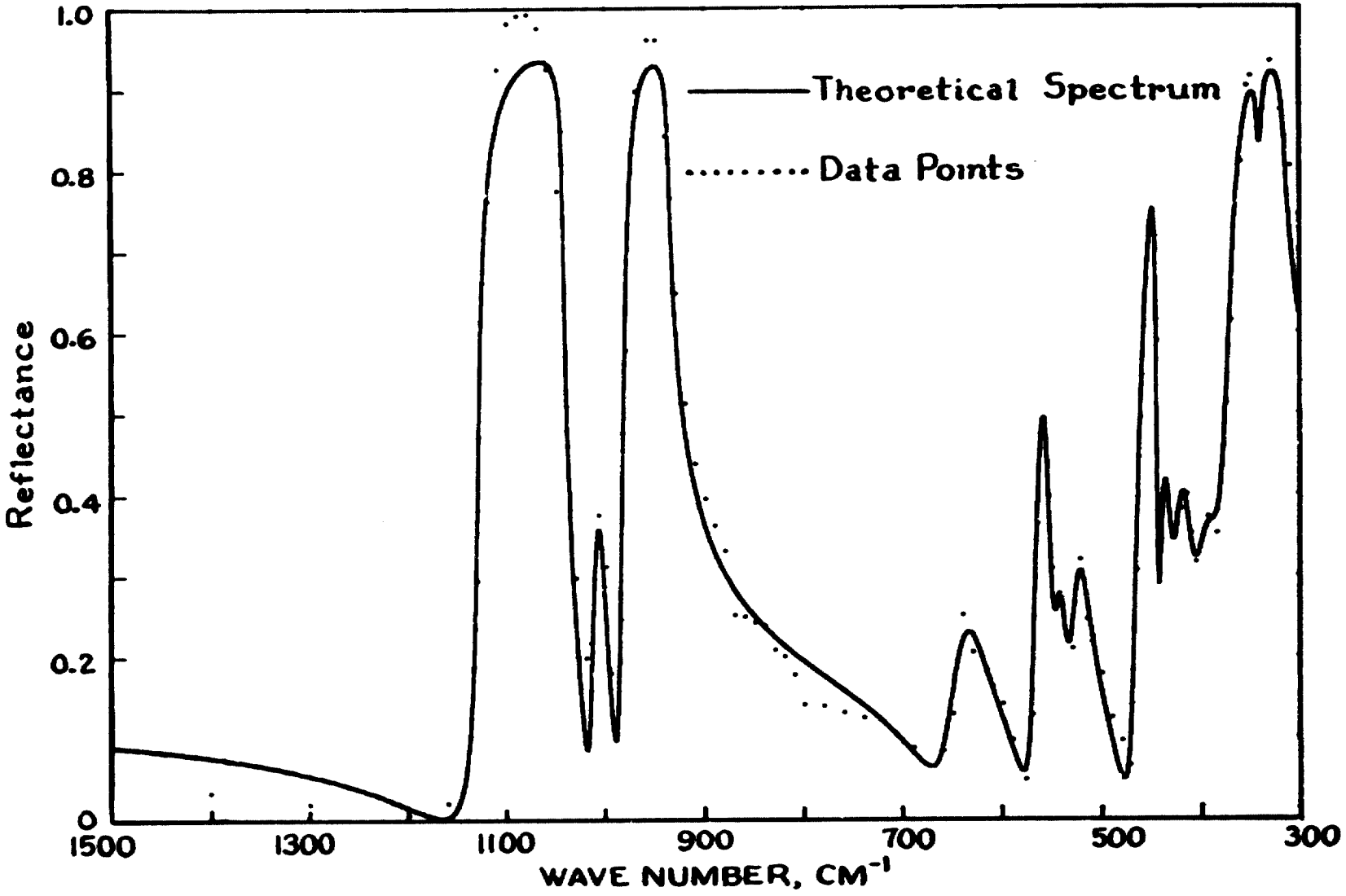

REFLECTANCE SPECTRUM OF ENSTATITE (E⊥a) FITTED WITH THIRTEEN LINES

Figure 4

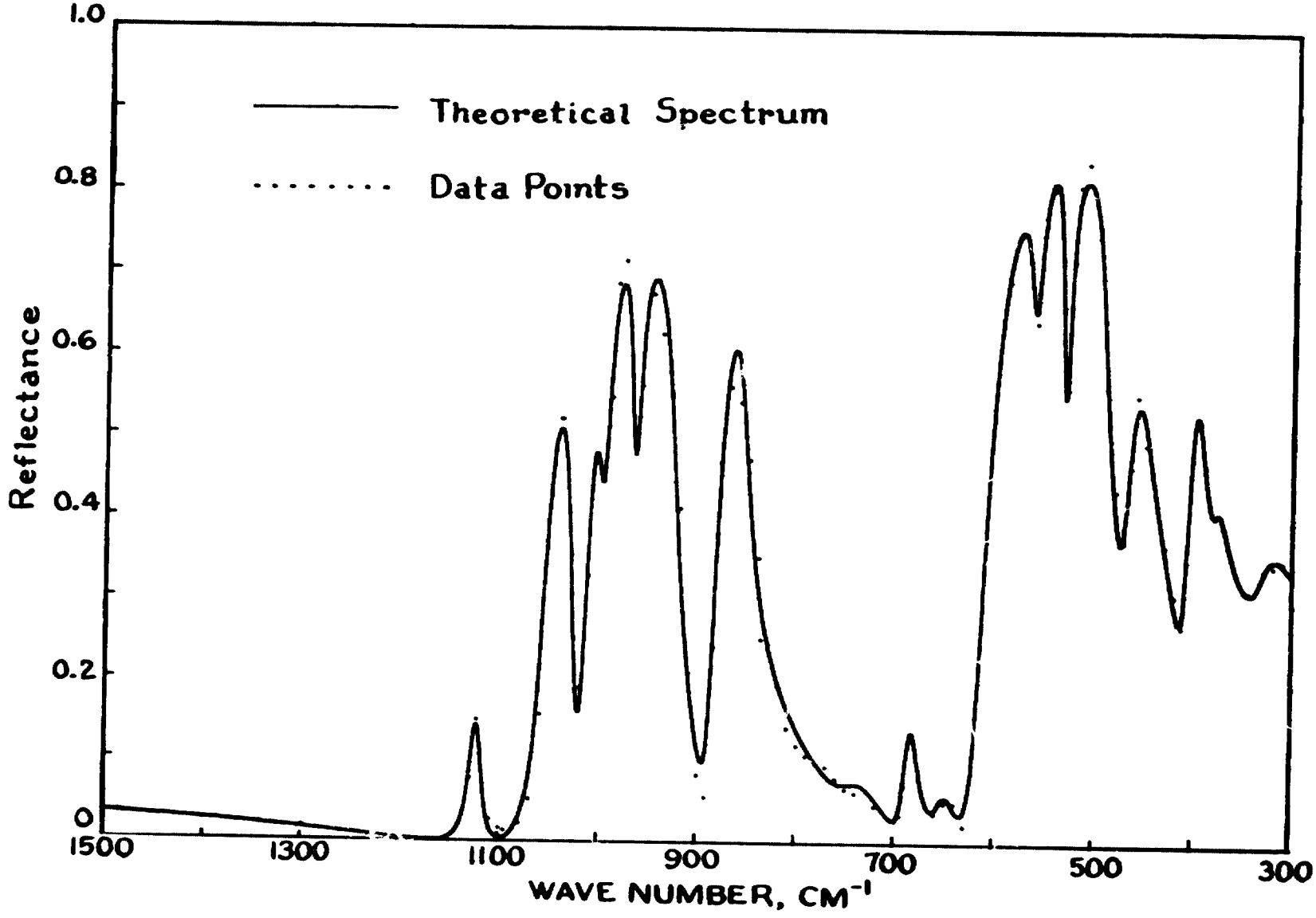

REFLECTANCE SPECTRUM OF ENSTATITE (E ⊥b) FITTED WITH SIXTEEN LINES

Figure 5

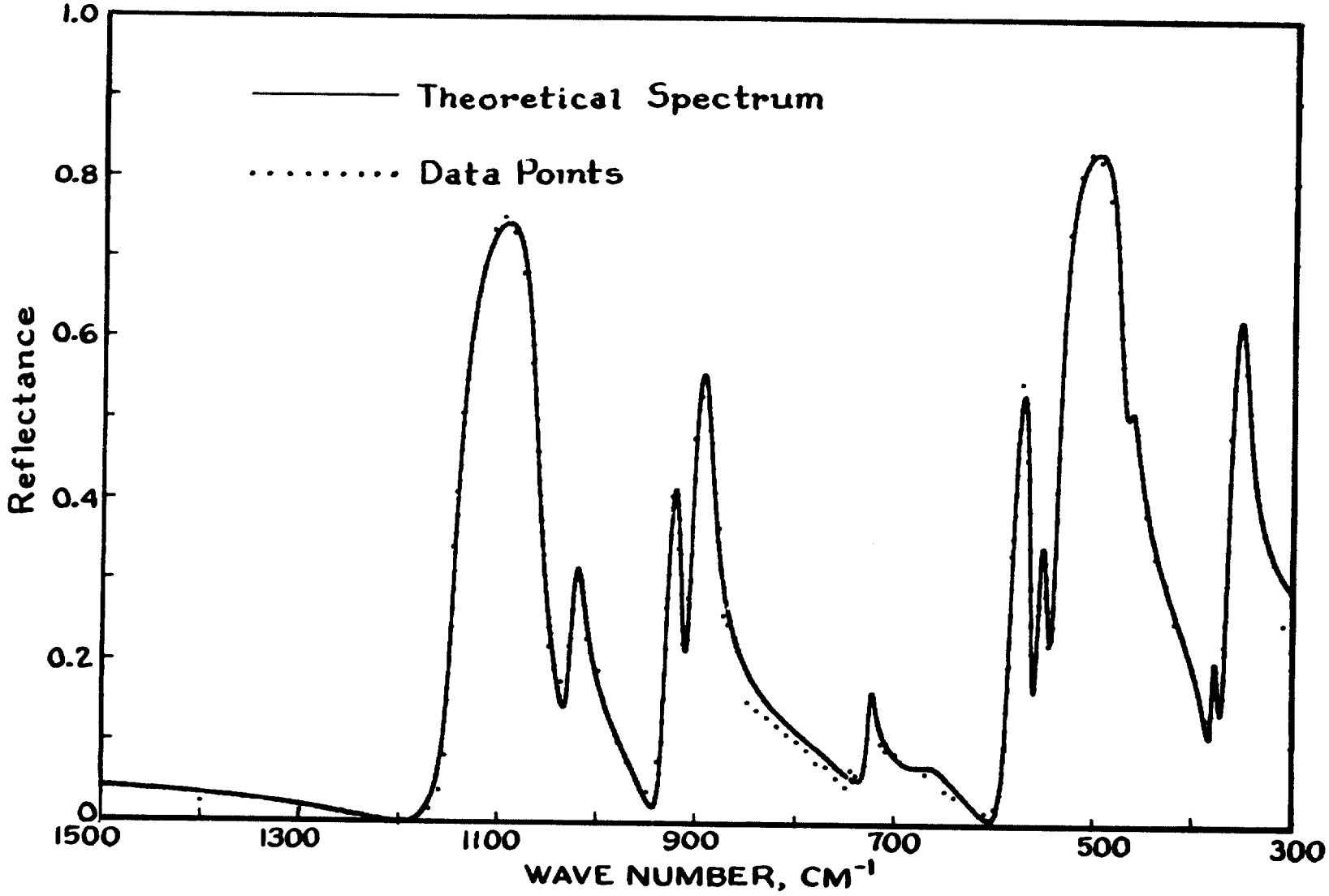

REFLECTANCE SPECTRUM OF ENSTATITE (E⊥c) FITTED WITH THIRTEEN LINES

Figure 6.

REFERENCES

1. J. R. Aronson and E. M. Smith, Mid Infrared Spectra of Lunar and Analog Soils, Proc. Lunar Sci. Conf. 9th, p 2911-2917 (1978).

2. D. S. McKay, private communication.

3. F. Chayes and D. Metais, Carnegie Institution Geophysical Laboratory Yearbook, p 193-195 (1963).

4. G. Heiken, A Catalog of Lunar Soils, National Aeronautics and Space Administration (1964).

5. R. V. Morris, Surface Exposure Indices of Lunar Soils: A Comparative FMR Study, Proc. Lunar Sci. Conf. 7th, p 315-335 (1976).

6. J. R. Aronson, E. M. Smith and P. F. Strong, Infrared Spectra of Lunar Soil Analogs, Final Report on Contract NASW-2918 (1977).